Cent. Eur. J. Chem. • 6(4) • 2008 • 555–561
DOI: 10.2478/s11532-008-0059-7

VERSITA

Central European Journal of **Chemistry**

# Density and Temperature Effect on Hydrogen-Bonded Clusters in Water - MD Simulation Study

**Research Article**

Dorota Swiatla-Wojcik*, Anna Pabis, Joanna Szala

*Institute of Applied Radiation Chemistry,*
*Technical University of Lodz,*
*90-924 Lodz, Poland*

**Received 9 May 2008; Accepted 21 July 2008**

**Abstract:** Molecular dynamics NVE simulations have been performed for five thermodynamic states of water including ambient, sub- and supercritical conditions. Clustering of molecules via hydrogen bonding interaction has been studied with respect to the increasing temperature and decreasing density to examine the relationship between the extent of hydrogen bonding and macroscopic properties. Calculations confirmed decrease of the average number of H-bonds per molecule and of cluster-size with increasing temperature and decreasing density. In the sub- and supercritical region studied, linear correlations between several physical quantities (density, viscosity, static dielectric constant) and the total engagement of molecules in clusters of size $k > 4$, $P_{k>4}$, have been found. In that region there was a linear relationship between $P_{k>4}$ and the average number of H-bonds per water molecule. The structural heterogeneity resulting from hydrogen bonding interactions in low-density supercritical water has been also discussed.

**Keywords:** *Hydrogen bonds • Supercritical water • Molecular clusters • MD simulation*



## 1. Introduction

The ability to form large molecular clusters, in which molecules are continuously connected via hydrogen bonds, is a characteristic feature of highly associated liquids. On the other hand, it is commonly known that macroscopic properties like viscosity, static dielectric constant, heat capacity, compressibility or diffusivity strongly depend on temperature and density of associated liquids. In particular the physicochemical and thus the solvent properties of water can rapidly change with increasing pressure and temperature [1,2]. Above the critical point ($T_c$ = 647.13 K, $\rho_c$ = 322 kg $m^{-3}$, $p_c$ = 22.055 MPa) water becomes highly compressible and diffusive. The static dielectric constant approaches values characteristic of low-polar solvents, even though the single water molecule remains polar. Unlike liquid water at ambient conditions, supercritical water is a poor solvent for ionic species, but is quite miscible with hydrocarbons and gases [1-3]. The ionic product of supercritical water can be a few orders of magnitude higher than in ambient water, with consequent effects on the kinetics and mechanisms of chemical reactions. Thus water, which, under ambient conditions, is a non-ionic and polar solvent, may become an ionic and low-polar solvent above the critical point. With adjustment of thermodynamic conditions, one can control viscosity, polarity or pH to obtain the desired solvent properties. This highly tuneable reaction medium has encouraged many technological applications, like hydrothermal synthesis or supercritical water oxidation [1].

An alteration in the character of water as a solvent near and above the critical point is thought to be a consequence of the structural transformations in the hydrogen-bonded network. As evidenced by many experimental and simulation studies the average number of hydrogen bonds per molecule and the lifetime of hydrogen bonds decrease with increasing temperature and decreasing density [3,4]. The temperature and the density limits for the existence of hydrogen bonds in water are not precisely known. High-temperature

* *E-mail: swiatlad@p.lodz.pl*

**Table 1.** The macroscopic properties of the thermodynamic states of water investigated.

| Label | T, K | T* a) | ρ, kg m$^{-3}$ | ρ* a) | $\varepsilon_s$ b) | η, μ Pa s b) |
|---|---|---|---|---|---|---|
| TS1 | 298 | 0.49 | 998 | 2.64 | 78.7 | 891 |
| TS2 | 573 | 0.94 | 720 | 1.90 | 20.5 | 87 |
| TS3 | 623 | 1.02 | 610 | 1.61 | 14.3 | 71 |
| TS4 | 653 | 1.07 | 451 | 1.19 | 8.55 | 53 c) |
| TS5 | 673 | 1.10 | 167 | 0.44 | 2.51 | 29 |

*a) $T^* = T / T_c^{CF}$ and $\rho^* = \rho / \rho_c^{CF}$ ; b) the static dielectric constant and viscosity from the latest IAPWS Release (www.iapws.org), c) interpolated value.*

spectroscopy experiments have indicated that hydrogen bonding persists well above the critical temperature [4]. Neutron scattering studies have shown the existence of H-bonds in supercritical water at densities as low as 200 kg m$^{-3}$ [5]. The remnant hydrogen-bonded network in supercritical water takes the form of finite-size molecular clusters. Size and topology of the hydrogen-bonded clusters had been investigated for various thermodynamic states by computer simulations [4,6] but a relationship between the extent of hydrogen-bonded clustering and the macroscopic properties of water was not specified.

The aim of this paper is to examine the effects of temperature and density on the connectivity of hydrogen bonds and to link features of hydrogen bonding with the observed macroscopic properties. Molecular dynamic simulations have been performed to generate water structures for the five thermodynamic states listed in Table 1.

The point TS1 is at ambient conditions. The two thermodynamic states, TS2 and TS3, correspond to liquid water in the sub-critical region. The state TS2 is located very near the liquid-vapour coexistence curve. The other two points, TS4 and TS5, are in the supercritical region and represent dense and low-density fluid, respectively. A quantification of hydrogen-bonded pairs has been performed using the recently proposed extended energetic criterion, which takes account of the intermolecular interaction and separation, and the orientation of H-donating molecule [7].

## 2. Computational Details

The NVE molecular dynamics simulations were performed for water at the five thermodynamic conditions characterized in Table 1. The cubic box contained 400 water molecules. The simulated systems have been twice as large as those in previous studies [4,6]. At the high temperatures studied, intermolecular vibrational energies were comparable with $k_BT$. This indicates the need to use a flexible model of water that better captures distortion and breakage of the hydrogen-bonded network. All simulations were done using the 3-site BJH model [8]. The intermolecular part of the BJH potential is described by the the central force potential [9], which leads to the liquid-vapour coexistence curve and the critical point ($T_c^{CF}$ = 609.5 K, $\rho_c^{CF}$ = 378 kg m$^{-3}$, $p_c^{CF}$ = 27.5 MPa) [10]. The partial charges $q_O$ = -0.66*e* and $q_H$ = +0.33*e* located on the oxygen and hydrogen atoms, respectively, are smaller than those used in other models of water, e.g. SPC/E [11]. Smaller charges have been found to provide better descriptions of the high-temperature and low-density thermodynamic states [10]. The BJH model correctly reproduces the observed properties of liquid water: pair correlation functions, heat capacity, compressibility, self-diffusion coefficient, vibrational spectrum, and dielectric relaxation [12]. The gas-liquid shifts, the blue-shift of the bending mode and the red-shift of the stretching mode, are also correctly matched.

The equations of motion were solved using a Verlet algorithm. Long-range Coulomb interactions were treated by Ewald summation and the shifted-force method was used for short-range non-bonding interactions [13]. Stability of the integration method required the time step of 0.25 fs at 298 K and 0.1 fs otherwise. The resulting stability of the total energy was $\Delta E/E \sim 10^{-6}$. Both simulations were extended to 15 ps after the pre-equilibration stage of about 7 ps. Calculated trajectories of the system were recorded every 1 fs.

The H-bond criterion used in the investigation of the thermodynamic conditions involves the interaction energy *E*, the distance between the hydrogen atom of H-donor and the oxygen atom of H-acceptor $r_{O...H}$ , and the angle between the OH bond of the H-donor and the line connecting the oxygen atoms of two molecules $\alpha_{O...H-O}$ [7]:

$$\left.\begin{aligned} E &\le E^c \\ r_{O...H} &\le r_{OH}^c \\ \alpha_{O...H-O} &\le \alpha^c \end{aligned}\right\} \qquad (1)$$

The hybrid energy-distance criterion [4] was shown to overestimate the size of hydrogen-bonded clusters in conditions of high temperature and low density [7].

The H-bond energy threshold $E^c$ has been taken from the statistical distributions of the pair interaction energy

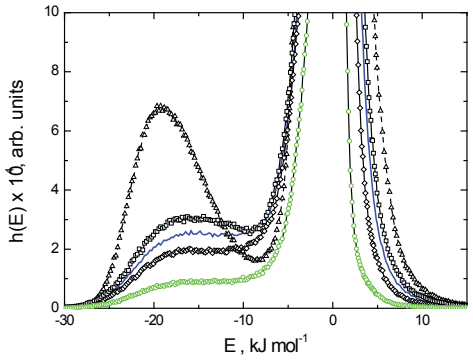


**Figure 1.** Normalized statistical distributions of pair interaction energy E in water calculated for the thermodynamic states listed in Table 1: TS1 (—Δ—), TS2 (—□—), TS3 (——), TS4 (—◇—), TS5 (—○—).

$E$ presented in Fig. 1. The assumed value of $E^c$ = -8 kJ mol$^{-1}$ delimits the low-energy part of strong attractive interactions in all of the systems studied. The allowable length of hydrogen bond $r_{OH}^c$ = 0.25 nm coincides with the minimum-position of the calculated $g_{OH}$ radial distribution functions (RDFs) shown in Fig. 2 and agrees well with the experimental scattering data [14]. The value of 30° has been adopted for $\alpha^c$. This assumption is consistent with the estimates for O-H…O angles derived from the X-ray Raman scattering experiments [15]. H-bonds were established in the simulation-generated configurations and a connectivity matrix for each configuration was determined. From the connectivity matrix molecules continuously connected by hydrogen bonds, can be easily separated into clusters. The H-bonded cluster was defined as consisting of molecules which have at least one H-bond to other members.

Connected molecules constitute clusters of varying size $k$. Considering $k$ as a random variable the probability density function of finding a given molecule in a H-bonded continuous cluster of size $k$ can be calculated as:

$$f_k = \frac{k}{N_{conf} \cdot N_{box}} \cdot N_k \qquad (2)$$

where $N_k$ is the number of clusters containing $k$ molecules, $N_{conf}$ denotes the number of sampled equilibrium configurations, and $N_{box}$ is the number of molecules in the simulation box. The probability density function $f_k$ can be converted into the cumulative distribution $F(N_{HB})$ via the relation:

$$F(N_{HB}) = \sum_{k=1}^{N_{HB}} f_k \qquad (3)$$

$F(N_{HB})$ represents the probability distribution function for a molecule to participate in a cluster of size $k \le N_{HB}$. The total engagement of molecules in the clusters composed of more than $N_{HB}$ molecules can be expressed as:

$$P(k > N_{HB}) = 1 - F(N_{HB}) = 1 - \sum_{k=1}^{N_{HB}} f_k \qquad (4)$$

The features of hydrogen-bonding, discussed below, represent the arithmetic mean of ten statistically-independent ensemble averages each resulting from $N_{conf}$ = 1000 equilibrium configurations.

## 3. Results and Discussion

Taking ambient water (TS1) as the reference system one can see features that imply the existence of hydrogen bonds in the states TS2 – TS5 as well as their progressive diminution with increasing temperature and decreasing density. Firstly, the distribution functions of the pair interaction energy in Fig. 1 exhibit a low-energy part from *ca.* -28 to -8 kJ mol$^{-1}$. The low-energy part evolves from a well–defined peak in ambient water to the shoulder seen for the supercritical state TS5.

Secondly, as shown in Fig. 2, the first maximum of the intermolecular $g_{OH}$ function precedes the maximum of the corresponding oxygen-oxygen RDF in all systems. Moreover, $g_{OH}$ shows O - H distances for neighbouring molecules between 0.1 and 0.25 nm, which is shorter than the sum of Van der Waals radii of the oxygen and hydrogen atoms of 0.27 nm. As can be seen, however, the height of the main peaks, $g_{OO}(R_{max})$ and $g_{OH}(R_{max})$, is lower for other states than for ambient water, and the secondary peak of $g_{OO}$ at 0.45 nm, which arises from the characteristic tetrahedral arrangement of molecules in the hydrogen-bonded network, is not seen in TS2 - TS5.. This indicates a breakage of the tetrahedral network and a decrease in the average number of H-bonded neighbours in sub- and supercritical water.

Finally, hydrogen bonding is reflected in changes in the molecular geometry. It is well known that the hydrogen-bonded molecule has longer OH bonds, smaller bond angle and higher dipole moment than the isolated monomer. Molecules in all states examined exhibit these features. The average molecular geometry and dipole moment are presented in Table 2. The decrease in OH-bond length and in the dipole moment, and the increase in the HOH angle, which are apparent when going from ambient to supercritical conditions, indicate a reduction in hydrogen bonding. Similar trends were observed in neutron scattering studies [5].

The features discussed above characterize the degree of local hydrogen bonding, which is usually expressed as the number of H-bonds $n_{HB}$ formed by a given molecule.The average values $\langle n_{HB} \rangle$ are listed in Table 2 and the statistical distributions of molecules according to the number of H-bonded neighbours are presented in Fig. 3. As expected, the degree of local hydrogen bonding gradually decreases with increasing temperature and decreasing density of water. A loss of molecules participating in four or three bonds is

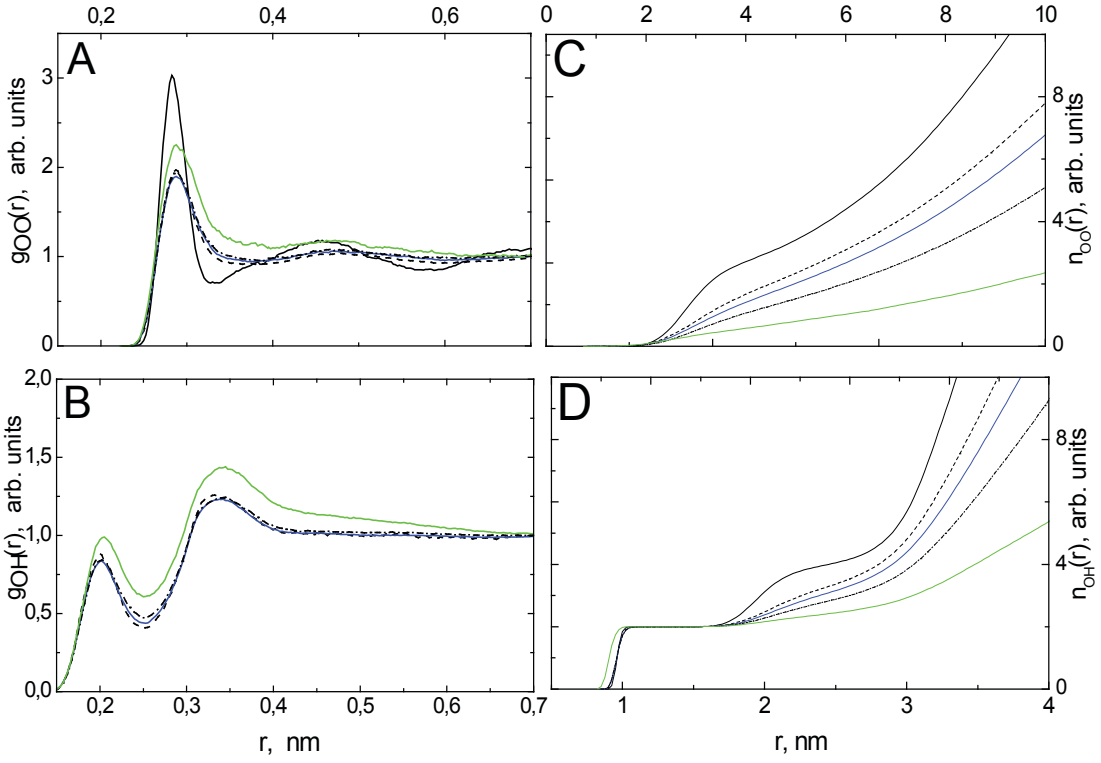


**Figure 2.** Oxygen-oxygen (A) and oxygen-hydrogen (B) radial pair distribution functions and the respective cumulative RDFs (C, D) calculated for water at temperatures and densities corresponding to the thermodynamic points TS1 (——), TS2 (– – –), TS3 (——), TS4 (— · —), TS5 (——).

**Table 2.** The calculated average properties of water molecules in the thermodynamic states studied: the bond length $l_{OH}$, bond angle $\theta_{HOH}$, dipole moment $\mu$ *) and the number of hydrogen-bonded neighbours $<n_{HB}>$. Size of the largest hydrogen-bonded cluster $(N_{HB})_{max}$ is given in the last column.

| State | $l_{OH}$, ($10^{-2}$ nm) | $\theta_{HOH}$ | μ, D | $<n_{HB}>$ | $(N_{HB})_{max}$ |
|---|---|---|---|---|---|
| TS1 | 9.75 ± 0.02 | 101.4° ± 0.03 | 1.97 ± 0.005 | 3.39 ± 0.02 | > 400 |
| TS2 | 9.75 ± 0.03 | 101.4° ± 0.04 | 1.96 ± 0.005 | 1.72 ± 0.02 | 336 ± 6 |
| TS3 | 9.74 ± 0.02 | 101.4° ± 0.03 | 1.95 ± 0.001 | 1.40 ± 0.03 | 199 ± 26 |
| TS4 | 9.73 ± 0.02 | 101.8° ± 0.02 | 1.94 ± 0.01 | 1.06 ± 0.02 | 62 ± 11 |
| TS5 | 9.70 ± 0.02 | 102.9° ± 0.01 | 1.91 ± 0.01 | 0.46 ± 0.02 | 15 ± 2 |

*) *The equilibrium geometry and dipole moment of the isolated molecule in the BJH model are: bond-length* $l^e_{OH}$ = 0.0957 nm, *bond-angle* $\theta^e_{HOH}$ = 104.5°, $\mu^e$ = 1.86 D.

associated with an increasing number of molecules having one or two H-bonded neighbours. In the low-density state TS5 the fraction of the latter is smaller than in the dense fluid (TS4) but not insignificant. The calculations show that 38.5% of molecules form at least one hydrogen bond. The presence of H-bonds at low densities agrees with the experimental reports: NMR [16], rapid X-ray diffraction [17], and neutron scattering [5].

We have found that the average number of hydrogen bonds per molecule near and above the critical point correlates linearly with the density, viscosity and static dielectric constant of states TS2 - TS5. On the other hand the macroscopic properties are supposed to be related to an extent of hydrogen-bonded interaction, i.e. to the assembly of H-bonded molecules into clusters. The effect of temperature and density on the extent of hydrogen-bonded clusters is illustrated in Fig. 4.

The cumulative distribution $F(N_{HB})$ calculated from eq. (3) shows the probability of finding a molecule in a cluster of size $k \leq N_{HB}$ as a function of $N_{HB}$. The largest cluster $(N_{HB})_{max}$ corresponds to point where $F(N_{HB})$ converges to unity. Values of $(N_{HB})_{max}$ are given in Table 2. In ambient water 99.9% of molecules exist in large clusters ($N_{HB} \geq 395$) and 0.1% constitute isolated monomers or dimers temporarily detached from the network. Interestingly, isolated trimers, tetramers, pentamers, *etc*. have not been found in TS1. Our result

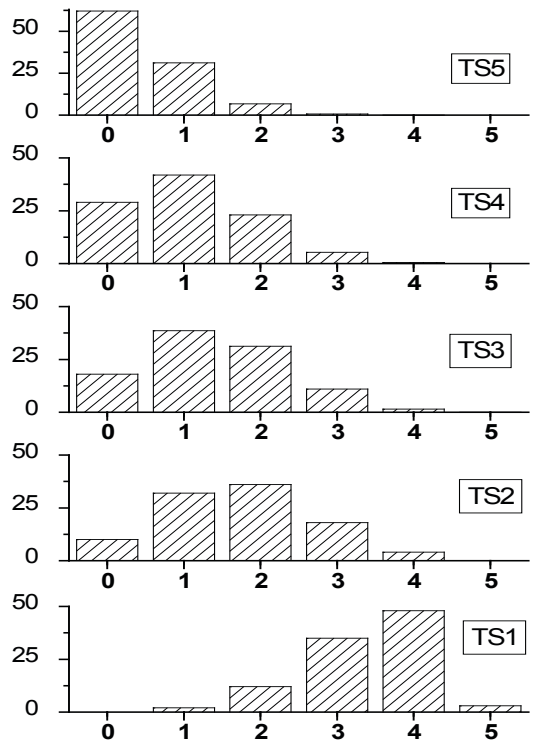


**Figure 3.** Percentage of water molecules forming i = 0, 1, 2, 3, 4, 5 hydrogen bonds calculated for the thermodynamic states listed in Table 1.

upgrades the size of large clusters in ambient water, which was estimated in the simulations with smaller model systems as $N_{HB}$ > 200 [4,6]. According to the percolation theory, the size of hydrogen-bonded clusters can be related to $<n_{HB}>$. Blumberg *et al*. estimated that if $<n_{HB}>$ exceeds the percolation threshold of 1.56 the interconnected molecules form a space-filling infinite H-bonded network [18]. In ambient water $<n_{HB}>$ = 3.4 is far above 1.56. This indicates the presence of an infinite network of H-bonds in accordance with the features exhibited by $F(N_{HB})$. Extensive connectivity is also observed in the liquid-vapour equilibrium state. The TS2 distribution shows continuous variety of clusters and reflects density fluctuations when the liquid is in coexistence with its vapour. There are about 340 hydrogen-bonded molecules in the largest cluster. The extensive connectivity is consistent with the value of $<n_{HB}>$ = 1.72, slightly exceeding the percolation threshold. Significant diminution of big clusters is seen in TS3 where the percolation threshold is not reached. A further diminution occurs in the supercritical region. The TS4 and TS5 distributions rapidly approach unity. This indicates the elimination of large clusters in favour of small ones. In the supercritical region, the cluster size is strongly affected by density. The most extensive cluster

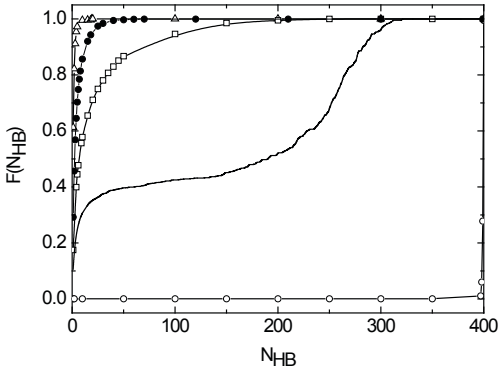


**Figure 4.** The cumulative distribution functions $F(N_{HB})$ for fraction of molecules belonging to the H-bonded cluster of size $N_{HB}$ calculated for the thermodynamic states TS1 (—○—), TS2 (——), TS3 (—□—), TS4 (—●—), TS5 (—Δ—).

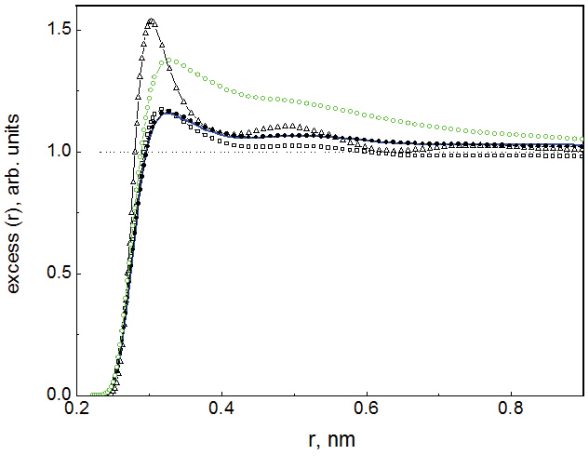


**Figure 5.** Excess of the local density defined in eq. (5) as a function of distance *r* from a central molecule: TS1 (—Δ—), TS2 (—□—), TS3 (——), TS4 (—●—), TS5 (—○—).

at 451 kg m$^{-3}$ and 653 K consists of 62 hydrogen bonded molecules whereas at 167 kg m$^{-3}$ and 673 K $(N_{HB})_{max}$ = 15. In the latter system, multi-molecular clusters show the branched-chain structure resulting in the relatively small $<n_{HB}>$. The persistence of clusters, however, even in this situation, suggests that aggregation of molecules prevails over the trend of equal space filling. We calculated an excess of the local density around a molecule in each system following the formula:

$$excess(r) = \frac{n_{OO}(r)}{\frac{4}{3}\pi\left(r^3 - r_0^3\right)\rho_n} \qquad (5)$$

In eq. 5 $n_{OO}(r)$ denotes the cumulative oxygen-oxygen radial distribution function, and $\rho_n$ is the number density of the system. The radius $r_0$ describes the outermost sphere around a molecule with no neighbour inside. Its value equals the largest distance at which $g_{OO}(r)$ = 0. The denominator in eq. (5) represents the expected number of molecules in a spherical shell with inner radius $r_0$ and outer radius *r,* under an assumption of equal space filling.

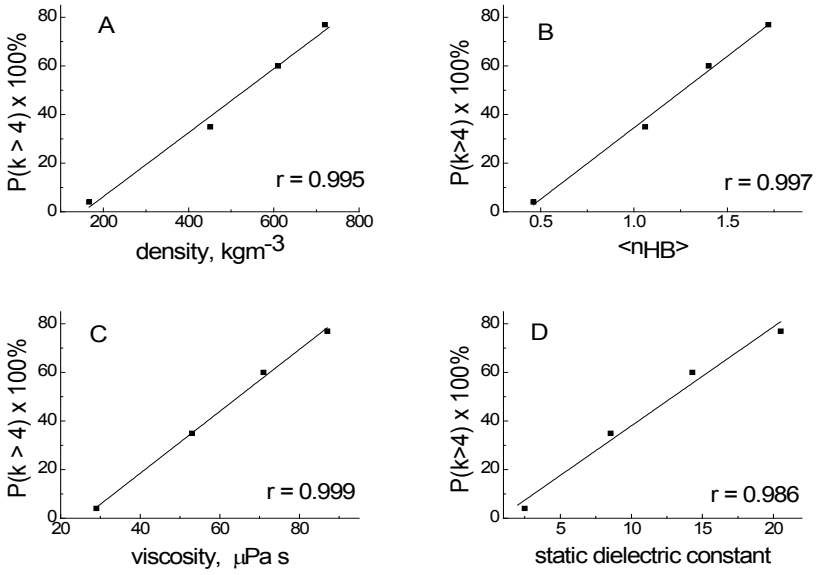


**Figure 6.** The probability $P(k > 4)$ as defined in eq. (4) and calculated for TS2–TS5 versus: (A) density, (B) the calculated average number of H-bonds per molecule $<n_{HB}>$, (C) viscosity, (D) static dielectric constant. Lines represent linear least squares fits. Correlation coefficients $r$ are given in the figure.

The *excess(r),* displayed in Fig. 5, describes the deviation from the expected number of molecules in each of the systems examined. The significant long-range excess seen for TS5 confirms aggregation of molecules and indicates the existence of density heterogeneity. Such a conclusion is consistent with the NMR observation that hydrogen bonding in supercritical water becomes spatially more inhomogeneous at lower densities [16]. It also validates the result of a small-scale simulation employing a different model of water [6].

To examine the relationship between the extent of hydrogen bonding and the macroscopic properties in the sub- and supercritical regions, we calculated the engagement of molecules in multi-molecular clusters. Definition of a multi-molecular cluster is somewhat arbitrary. However, taking into account that the water molecule is able to form four hydrogen bonds, the pentamer has been assumed to designate the smallest multi-molecular cluster. The engagement of molecules in clusters composed of at least five molecules, $P(k > 4)$, can be obtained from eq. (4) for $N_{HB} = 4$. In Fig. 6, values of $P(k > 4)$ calculated for TS2 – TS5 are plotted against the values of density, viscosity and static dielectric constant listed in Table 1. In each case - $P(k > 4)$ *vs.* density, $P(k > 4)$ *vs.* viscosity and $P(k > 4)$ *vs.* static dielectric constant – closely linear relationships have been found. The change of thermodynamic conditions from TS2 to TS5 reduces the engagement of molecules in multi-molecular clusters, which in turn results in the decreases in viscosity and dielectric constant. Fig. 6 also shows a linear dependence between $P(k > 4)$ and $<n_{HB}>$, which explains the correlations found between $<n_{HB}>$ and the experimental density, viscosity and dielectric constant. These results give preliminary grounds for the use of $<n_{HB}>$ as an indicator of structural transformations in the hydrogen-bonded network, and of the consequent changes of macroscopic properties. Further studies including simulations of other thermodynamic states and calculation of the dynamical and dielectric properties are in progress. The observed effects of temperature and density on the connectivity of hydrogen bonds is qualitatively the same as reported in the simulations of smaller systems [4,6]. However, the cluster statistics is significantly dependent on the number of molecules in the simulation box. The distribution functions $F(N_{HB})$ obtained in the present work are broader because clusters tend to be larger with increasing $N_{box}$. Our results are more consistent with the percolation theory than those of the less extended simulation [6]. The correlations discussed above are not expected to be particularly sensitive to system size, because the development of $F(N_{HB})$ with increasing $N_{box}$ proceeds similarly in all thermodynamic states.

## 4. Conclusions

Multi-molecular hydrogen bonded clusters have been found in all of the thermodynamic states of water studied. The size of clusters and the average number of H-bonds per molecule $<n_{HB}>$ decrease with increasing temperature and decreasing density. The observed trends are qualitatively the same as reported in smaller-

scale simulations but the clusters are larger in size. In the low-density supercritical water branched-chain clusters of H-bonded molecules are incorporated into molecular aggregates, resulting in density heterogeneities.

In the sub- and supercritical region (states TS2 - TS5 in Table 1) studied, variations in the total engagement of molecules in clusters composed of at least five molecules is related to changes in the experimental density, static dielectric constant and viscosity. A linear correlation between molecular engagement in these clusters and $<n_{HB}>$ has been also found. This result gives preliminary grounds for the use of $<n_{HB}>$ as an indicator of structural transformations in the hydrogen-bonded network, and of consequent changes in the macroscopic properties in the region explored.

## References


[1] E. Kiran, P. G. Debenedetti, C. J. Peters (Eds); Supercritical Fluids. Fundamentals and Applications, NATO Science Series E: Applied Science – vol. 366 (Kluwer Academic Publishers, 2000)

[2] D. A. Palmer, R. Fernandez-Prini, A. H. Harvey (Eds); Aqueous Systems at Elevated Temperatures and Pressures (Elsevier, 2004)

[3] A. Kruse, E. Dinjus, J. Supercritical Fluids, 39, 362 (2007)

[4] A. G. Kalinichev, In: R. T. Cygan, J. D. Kubicki (Eds); Reviews in Mineralogy and Geochemistry, vol. 42 (Mineralogical Society of America, Washington D. C., 2001) 83

[5] M.-C. Bellissent-Funel, J. Mol. Liq. 90, 313 (2001)

[6] R. D. Mountain, J. Chem. Phys. 110, 2109 (1999)

[7] D. Swiatla-Wojcik, Chem. Phys. 342, 260 (2007)

[8] P. Bopp, G. Jancso, K. Heinzinger, Chem. Phys. Lett. 98, 129 (1983)

[9] F. H. Stillinger, A. Rahman, J. Chem. Phys. 68, 666 (1978)

[10] B. Guillot, Y. Guissani, J. Chem. Phys. 108, 10162 (1998)

[11] H. J. C. Berendsen, J. R. Grigera, T. P. Straatsma, J. Phys. Chem. 91, 6269 (1987)

[12] I. Ruff, D. J. Diestler, J. Chem. Phys. 93, 2032 (1990)

[13] M. P. Allen, D. J. Tildesley; Computer Simulation of Liquids (Oxford University Press, Oxford, 1987)

[14] T. Head-Gordon, G. Hura, Chem. Rev. 102, 2651 (2002)

[15] Ph. Wernet, D. Testemale, J.-L. Hazemann, R. Argoud, P. Glatzel, L. G. M. Pettersson, A. Nilsson, U. Bergmann, J. Chem. Phys. 123, 154503 (2005)

[16] N. Matubayasi, C. Wakai, M. Nakahara, J. Chem. Phys. 107, 9133 (1997)

[17] T. Yamaguchi, J. Mol. Liq. 78, 43 (1998)

[18] R. L. Blumberg, H. E. Stanley, A. Geiger, P. Mausbach, J. Chem. Phys. 80, 5230 (1984)